THE JOURNAL OF PHYSICAL CHEMISTRY Letters

Letter

pubs.acs.org/JPCL

Correlated Local Bending of a DNA Double Helix and Its Effect on DNA Flexibility in the Sub-Persistence-Length Regime

Xinliang Xu,[†,‡] Beng Joo Reginald Thio,[‡] and Jianshu Cao*[,†,§]

[†]Department of Chemistry, Massachusetts Institue of Technology, Cambridge, Massachusetts 02139, United States

[‡]Pillar of Engineering Product Development, Singapore University of Technology and Design, 20 Dover Drive, 138682 Singapore

[§]Singapore−MIT Alliance for Research and Technology (SMART), 1 Create Way, #10-01 Create Tower, 138602 Singapore

Supporting Information

ABSTRACT: Mechanical characteristics of DNA in the sub-persistence-length ($l_P \approx$ 150 base pairs) regime are vital to many of its biological functions but not well understood. Recent experimental studies in this regime have shown a dramatic departure from the traditional worm-like chain model, which is designed for long DNA chains and predicts a constant flexibility at all length scales. Here, we report an improved model with explicit considerations of a new length scale $l_D \approx$ 10 base pairs, over which DNA local bend angles are correlated. In this correlated worm-like chain model, a finite length correction term is analytically derived, and DNA flexibility is found to be contour-length-dependent. While our model reduces to the traditional worm-like chain model at length scales much larger than l_P, it predicts that DNA becomes much more flexible at shorter sizes, in good agreement with recent cyclization measurements of short DNA fragments around 100 base pairs.

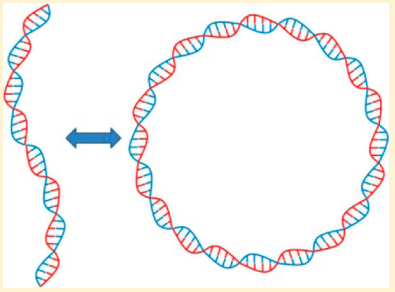

SECTION: Biophysical Chemistry and Biomolecules

The flexibility of DNA has great impacts on its overall shape as well as on many of its biological functions, such as chromosomal DNA packaging,[1] DNA damage repair,[2] regulation of gene expression,[3] and protein−DNA binding.[4] Many experimental techniques[5] and theoretical descriptions[6] have been developed to investigate the structural details of DNA underlying its mechanical characteristics. At very small length scales with atomic resolution, DNA is well studied from X-ray crystallography and NMR spectroscopy in conjunction with computer simulations.[7] At much larger length scales, experimental investigations of long DNA of more than 1000 base pairs (bps) have supported the worm-like chain (WLC) model,[8] where DNA is described as a continuous semiflexible polymer with all local details coarse-grained into one parameter, the persistence length $l_P \approx$ 150 bps.[9,10] However, for a wide range of problems of biological significance, the length scale of importance falls in between the atomistic description and the continuous description. Experiments are now beginning to bridge the gap, and the newly observed DNA mechanical properties at these intermediate length scales strongly challenge the application of the WLC model.[11−13] Here, we propose a more comprehensive model by incorporating structural details of DNA underlying these newly observed mechanical properties.

The development of the WLC model starts from a discrete description of DNA, constructed by linking successive equal-sized segments with length l_0, pointing to the direction $\vec{t}_i$ for the ith segment (Figure 1A). In 3D, we use $\vec{b}_i \equiv \theta_i \hat{n}_i$ to characterize local bending between the ith and the $(i+1)$th segments with respect to the local axis $\hat{n}_i \equiv \vec{t}_i \times \vec{t}_{i+1}$, with amplitude $\cos\theta_i = \vec{t}_i \cdot \vec{t}_{i+1}$. In the most naïve Freely Jointed Chain (FJC) model, these segments are considered as uncorrelated, that is, $\langle \vec{t}_i \cdot \vec{t}_{i+1} \rangle = \delta_{ij}$, where δ_{ij} is the Kronecker delta function. As an improved description, the Kratky−Porod (KP) model[14] assumes that DNA resists to bending deformation, characterized by an elastic energy of bending defined through

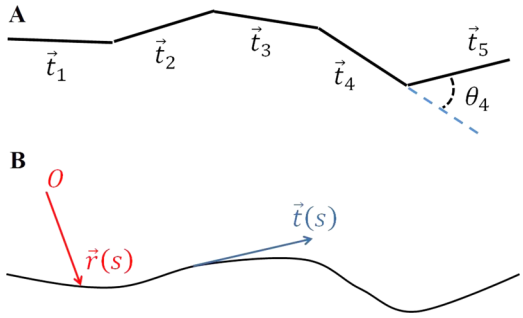

Figure 1. Description of the WLC model. (A) Illustration of the KP model. (B) Illustration of the WLC model.

$$E_{KP} = \frac{B}{l_0}\sum_{i=1}^{N-1}(1 - \vec{t}_i\cdot\vec{t}_{i+1}) = \frac{B}{l_0}\sum_{i=1}^{N-1}(1 - \cos\theta_i) \quad (1)$$

where $B = l_P k_B T$ is the bending modulus. Building upon this assumption, it can be shown that the orientations of different

Received: June 24, 2014
Accepted: August 5, 2014
Published: August 5, 2014

   dx.doi.org/10.1021/jz501290b | J. Phys. Chem. Lett. 2014, 5, 2868−2873

chain segments are correlated such that $\langle \vec{t}_i \cdot \vec{t}_{i+1} \rangle = e^{-l_0|i-j|/l_P}$. The WLC model is obtained by taking the continuous limit ($l_0 \to 0$, $N \to \infty$, with $Nl_0 = L$) of eq 1 as

$$E_{WLC} = \frac{B}{2} \int_0^L \left(\frac{d\vec{t}}{ds} \right)^2 ds \tag{2}$$

where the DNA chain is fully described by a continuous chain (Figure 1B) parametrized by s with unit tangent vector $\vec{t}(s)$ and bending is characterized locally by the change of chain tangent $d\vec{t}/ds$. Correspondingly, the tangent vectors at different chain locations are correlated such that $\langle \vec{t}(s_1) \cdot \vec{t}(s_2) \rangle = e^{-|s_1-s_2|/l_P}$. Calculations based on this continuous description (eq 2) show excellent agreement between theory and experiment for long DNA chains of $L \gg l_P$. For example, the experimentally observed force-extension behavior of a long DNA chain of contour length of about 100 000 bps[15] fits extremely well with the WLC prediction[8,16] at persistence length $l_P = 53$ nm.

However, the agreement between the WLC model and the classical force-extension measurements at long chain limit cannot unveil any information about local bend angle distribution at short length scales because at the long chain limit, the iterated convolution of any arbitrary local bend angle distribution with itself always converges to a Gaussian form, as predicted by the WLC model. While there is no experimental evidence supporting the direct extrapolation of WLC to short length scales, recent experimental studies of DNA ring-closure probability in the sub-persistence-length regime show significant "softening" of DNA[12,17] and challenge the application of the WLC model under two extreme conditions, short length scales as well as strong bending. Previous efforts for improving the WLC model have focused on strong bending and proposed the introduction of new structural features (e.g., bubbles,[18] kinks,[19] or subelastic modes[20]) that lower the bending energy from quadratic to a softer form beyond a critical curvature. While the response of DNA upon strong bending is an active field of research, systematic estimation of the critical curvature leads to a DNA mini-circle of contour length $L^* \sim 70$ bps.[21] This estimate is considerably smaller than the contour lengths[12,17] at which the softening behavior of DNA is observed, rendering strong bending irrelevant and suggesting additional mechanisms at work. Furthermore, experiments on short DNA fragments in the weakly bending limit also indicate the WLC model to be insufficient and suggest a length-dependent DNA flexibility.[13] We believe that these measurements provide the exact data needed to investigate the local bend angle distribution and propose an improved description of DNA by considering the effect of a newly observed[4] and studied[22] feature, the interaction between local deformations. According to these recent studies, upon a local deformation, all units of the mechanical network of DNA have to relocate until force balance is restored, resulting a structural change that is no longer local but propagates along the DNA chain with a new length scale $l_D \approx 10$ bps, manifested in the form of allosteric protein binding through DNA.[22] Here, we assume that there exists a similar interaction between local bending deformations so that the bending energy (eq 1) that the KP model is built upon, where local bend angles are treated as independent, is only valid for $l_0 \gg l_D$. Then, the WLC predictions, obtained at large N limit as the continuous limit of the KP model, only apply for sufficiently long DNA chains as $L = Nl_0$. For shorter chains of interest, the interaction between local bend angles needs to be incorporated into the definition of a more general bending energy. Because the details about bending at the shortest length scale (bp level) are still not available, here in our correlated WLC (C-WLC) model, the system is coarse-grained at a length scale l_0 comparable to l_D, and the bending energy is approximated by truncation of interactions beyond nearest-neighbor bend angles

$$E_{C\text{-}WLC} = \frac{B'}{2l_0} \sum_i \left(\theta_i^2 + \frac{2C\vec{b}_i \cdot \vec{b}_{i+1}}{1 + C^2} \right) \equiv k_B T \sum_{i,j} \boldsymbol{A}_{ij} \vec{b}_i \cdot \vec{b}_j \tag{3}$$

where $B' = l'_P k_B T(1 + C^2)/(1 - C^2)$ is the local bending modulus, which is shown to be related to l_P later, and C is the coupling strength. This more generally defined bending energy predicts a correlated distribution of $\{\vec{b}_i \equiv \theta_i \hat{n}_i\}$ as a multivariate Gaussian characterized by covariance matrix $\boldsymbol{A}^{-1}$ such that $\langle \vec{b}_i \cdot \vec{b}_j \rangle = (\boldsymbol{A})^{-1}_{ij}$. In the case of the simple tridiagonal Toeplitz matrix $\boldsymbol{A}$, the inverse can be analytically obtained as $(\boldsymbol{A})^{-1}_{ij} = (2l_0/l'_P) \times (-C)^{|i-j|}$ (see the Supporting Information (SI) for the derivation), resulting in an additional short-range correlation for the binormal vector $\vec{b}(s) = \vec{t}(s) \times (d\vec{t}/ds)(s)$ as $\langle \vec{b}(s_1) \cdot \vec{b}(s_2) \rangle \approx e^{-|s_1-s_2|/l_D}$, which is absent in the WLC model.

In an approximate but simple way, the flexibility of a C-WLC can be quantitatively studied by mapping it to a WLC of the same contour length with an effective persistence length l_{EP}, so that earlier analytical results can apply.[23−25] For a DNA chain of contour length $L = (N + 1)l_0$, the mapping can be done by matching the end-to-end tangent correlations. In our C-WLC model, the end-to-end tangent correlation is (see the SI for derivation)

$$\begin{aligned} \langle \vec{t}_1 \cdot \vec{t}_{N+1} \rangle_{C\text{-}WLC} &= \left(\frac{1 - \langle \theta_i^2 \rangle}{2} \right)^N \times (1 - \langle \vec{b}_i \cdot \vec{b}_{i+1} \rangle)^{N-1} \\ &= e^{-Nl_0[1-((N-1)/N)2C]/l'_P} \end{aligned} \tag{4}$$

For a WLC with effective persistent length l_{EP}, the end-to-end tangent correlation is

$$\langle \vec{t}(0) \cdot \vec{t}(Nl_0) \rangle_{WLC} = e^{-Nl_0/l_{EP}} \tag{5}$$

A comparison between eqs 4 and 5 shows that the effective WLC has a contour-length-dependent persistence length

$$l_{EP}(L) = l'_P \left(1 - \frac{N-1}{N} 2C \right)^{-1} \xrightarrow{L \to \infty} l'_P (1 - 2C)^{-1} \tag{6}$$

From eq 6, we see that the effective persistence length $l_{EP}(L)$ approaches its long chain limit quickly as $N = L/l_0 - 1$ increases. At this long chain limit ($L \gg l_0 \approx 10$ bps), our C-WLC model can be reduced to the WLC model by setting $l_{EP}(\infty) = l'_P(1 - 2C)^{-1} = l_P$. For a short chain, our model introduces a correction term and predicts a contour-length-dependent persistence length

$$l_{EP}(L) = l_P \times \left(1 + \frac{2Cl_0}{(1 - 2C)L} \right)^{-1} \tag{7}$$

which is illustrated in Figure 2 by setting $2Cl_0/(1 - 2C) = 15$ bps.

The predictions from our C-WLC model may be compared to the recent J factor measurements of the probability of DNA forming a ring, defined as the ratio of equilibrium constants for cyclization and bimolecular association.[26] These results have been previously compared to theoretical predictions, obtained

dx.doi.org/10.1021/jz501290b | J. Phys. Chem. Lett. 2014, 5, 2868−2873

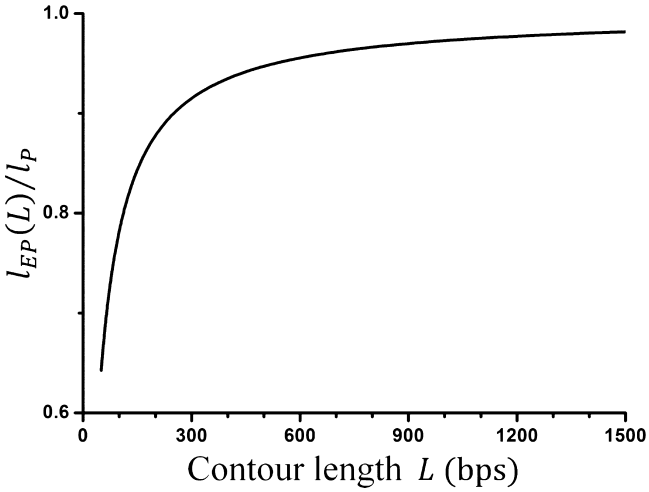

Figure 2. Contour-length-dependent persistence length. The flexibility of a C-WLC, characterized by a persistence length $l_{EP}(L)$, is a function of the contour length L.

by Shimada and Yamakawa in their seminal paper[23] where DNA is modeled as a twisted WLC (TWLC). In this detailed variation of the WLC model, the twist degree of freedom is considered explicitly by introducing an additional independent parameter, the twisting persisitence length l_T. With the local orientation of the DNA segment at $\vec{r}(s)$ described by an orthonormal triad $\vec{e}_i(s)$ $(i = 1-3)$, where $\vec{e}_3(s) = \vec{t}(s)$ is the tangent of the chain contour, the corresponding torsional energy can be written as $E_{\text{Torsion}} = 0.5 l_T k_B T \int_0^L (\omega_3 - \tau)^2 \, ds$, where $\omega_3(s) = \vec{\omega}(s) \cdot \vec{e}_3(s)$ is the local twist with $\vec{\omega}(s)$ determined from the relationship $d\vec{e}_i(s)/ds = \vec{\omega}(s) \times \vec{e}_3(s)$ and τ is the intrinsic twist. The J factor, $J_{\text{TWLC}}(L/l_P,\eta,\tau)$, is then obtained in terms of three parameters, L/l_P, $\eta \equiv l_P/l_T - 1$, and τ. It has been shown[6,17] that the experimentally observed J factors at shorter contour lengths can fit well to this theoretical prediction but as a softer WLC with $l_P = 47$ nm, $\eta = -0.2$, and $\tau = 2\pi/10.5 = 0.6$. Because l_P in the WLC model is an intrinsic parameter that is a constant at all length scales, the difference between $l_P = 53$ nm obtained at the long chain limit and $l_P = 47$ nm obtained at shorter length scales should not be overlooked.

Here, we attempt to resolve this difference and explain the short chain behavior using our C-WLC model. To highlight the effect of the new feature introduced in our model, for the J factor problem, we minimize the number of free parameters by fixing $\eta = -0.2$ and $\tau = 0.6$. Our C-WLC model then predicts the J factor as

$$J_{\text{C-WLC}}(L) = J_{\text{TWLC}}(L/l_{\text{EP}}(L), -0.2, 0.6) = J_{\text{TWLC}}\left(\left(L + \frac{2Cl_0}{1-2C}\right)/l_P, -0.2, 0.6\right) \quad (8)$$

Equations 7 and 8 show that, in addition to the persistence length l_P for an infinitely long chain, our model derives another free parameter, the finite length correction $l_c = [2Cl_0/(1 - 2C)]$. Here, we fix $l_P = 53$ nm because it is obtained at the long chain limit and fit the J factor measurements[17,27,28] to our theoretical predictions (eq 8) with a single parameter, the finite length correction l_c. A good fit is obtained at $l_c = [2Cl_0/(1 - 2C)] = 15$ bps, and our theoretical predictions show a significant enhancement in terms of the J factor over the WLC predictions for short chains (Figure 3A).

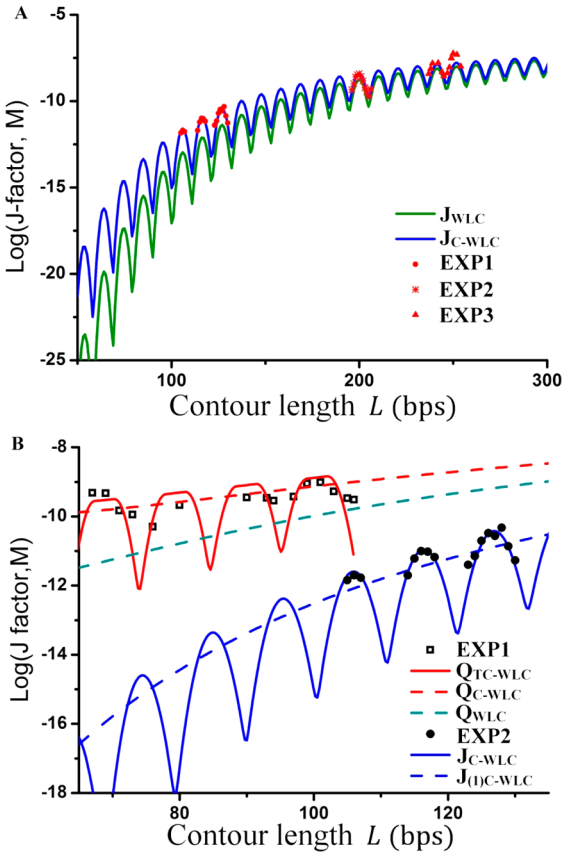

Figure 3. Ring closure probability (J factor) as a function of the contour length. (A) The experimental data taken from Du et al.[17] (red circles), Vologodskaia and Vologodskii[27] (red asterisks), and Shore and Baldwin[28] (red triangles) are compared with the WLC predictions (green solid line) and our C-WLC predictions (blue solid line). (B) The experimental data taken from Du et al.[17] (solid black circles) are compared with our C-WLC predictions $J_{\text{C-WLC}}$ when torsional alignment is considered (blue solid line) and $J_{(1)}$ when torsional alignment is not considered (blue dashed line). The experimental data for a finite capture radius R taken from Vafabakhsh and Ha[12] (open black squares) are compared to the theoretical predictions of Q_{WLC} (green dashed line), $Q_{\text{C-WLC}}$ (red dashed line), and $Q_{\text{TC-WLC}}$ (red solid line) at fixed capture radius $R = 6$ nm. DNA parameters used in both the WLC model and C-WLC model include $l_P = 53$ bps, $\eta = -0.2$, $\tau = 0.6$, and helical pitch $H = 10.5$ bps $= 3.57$ nm, while the C-WLC model has one more parameter, the finite length correction $l_c = 15$ bps.

Despite that our model predicts a much higher flexibility for short DNA chains, it still falls short in explaining the recent experimental observations by Vafabakhsh and Ha,[12] which reported a J factor about 3 orders of magnitude larger than the classical results by Du et al.[17] at the same contour length of $L = 105$ bps (Figure 3B). In this work,[12] Vafabakhsh and Ha argued that there may exist a capture radius, that is, instead of measuring the ring closure probability, their results correspond to the probability of the two DNA ends being separated by a distance R. This probability has been evaluated[29] within the WLC framework without consideration of the twist degree of freedom. However, the result $Q_{\text{WLC}}(L/l_P,R/L)$ (eq 21 in ref 29) still fell short in explaining the high flexibility observed.[12] While the underlying mechanism is an issue under heated debate,[21,30] here, we show that by replacing l_P with the contour-length-dependent persistence length $l_{\text{EP}}(L)$ with the same correction $l_c = 15$ bps, the modified function $Q_{\text{C-WLC}}$ significantly enhances

dx.doi.org/10.1021/jz501290b | J. Phys. Chem. Lett. 2014, 5, 2868−2873

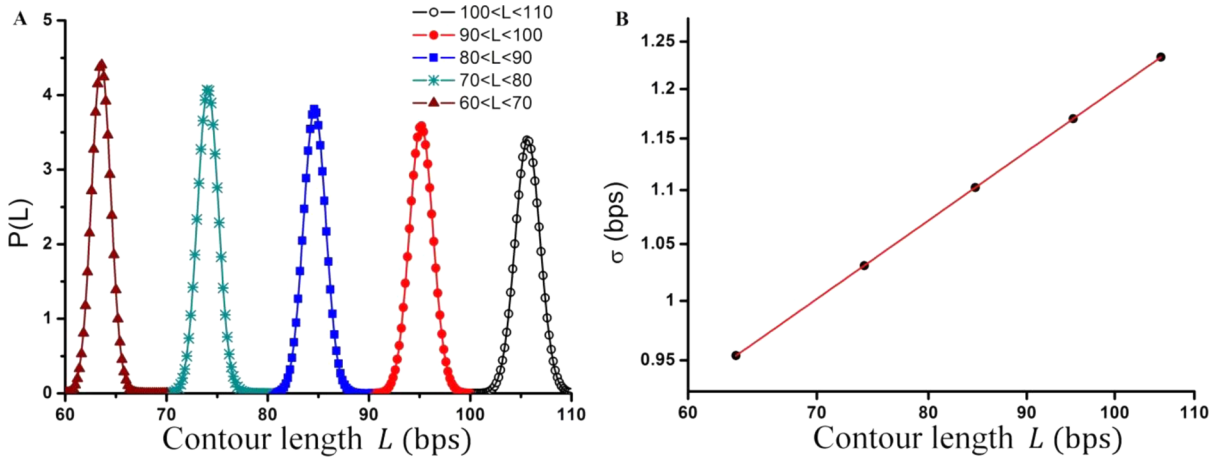

Figure 4. Contribution of the twist degree of freedom. (A) The results (symbols) of the ratio $P(L) \equiv J_{\mathrm{TWLC}}(L/l_{\mathrm{P}},-0.2,0.6)/J_{(1)}(L/l_{\mathrm{P}})$ fit well to a Gaussian function (line) in each color-coded region. (B) The standard deviations and the corresponding center locations (black circles), obtained from the Gaussian fits in (A), fit well to a linear function (red line) with slope $a = 0.505$ and intercept $b = -0.931$ in a logarithm−logarithm plot.

the resulting probability over the WLC result and matches qualitatively with the experimental measurements at $R = 6$ nm (Figure 3B).

The oscillatory behavior displayed by the measurements[12] suggests a certain degree of torsional alignment of the two DNA ends, which can be interpreted by including the twist degree of freedom into the theoretical consideration. In an approximate but simple treatment, we assume that at short length scales, the number of microstates that deviate strongly from the most probable configuration is negligibly small. This approximation suggests that the contour and twist degrees of freedom are decoupled. Using the mini-circle formed by DNA (orientation described by $\vec{e}_i(s)$ for $i = 1-3$ or the equivalent Euler angles $\vec{\Omega}(s) = [\theta,\phi,\psi]$) as an example, with the contour degree of freedom "frozen" at configuration $\{\vec{t}^*(s)\}$ (a circle of radius $L/2\pi$), we have $J_{\mathrm{TWLC}}(L) = J_{(1)}(L) \times P(L)$, where $J_{\mathrm{TWLC}}(L)$, the J factor with torsional alignment, can be obtained as the simple product of contour contribution $J_{(1)}(L)$ and twist contribution $P(L)$. Here, the twist contribution is modeled as the normalized probability density at torsional alignment, $P(L) \equiv 2\pi f[\gamma^*(L)]/\int_{-\pi}^{\pi} f(\gamma)\,\mathrm{d}\gamma$, where $f(\gamma)$ denotes the probability density associated with any total twist deformation of γ, and γ^* is the total twist deformation needed in order to have torsional alignment. Assuming that $f(\gamma)$ is dominated by the lowest twisting energy configuration, where the total twist deformation is evenly distributed along the chain ($\omega_3(s) - \tau = \gamma/L$), in our model, we have $f(\gamma) = \mathrm{e}^{-(l_{\mathrm{T}}/2L)\gamma^2}$. Furthermore, as the contour degree of freedom is "frozen" at $\{\vec{t}^*(s)\}$, γ^* can be obtained as

$$\begin{aligned}\gamma^*(L) &= \int_0^L (\omega_3(s) - \tau)\,\mathrm{d}s \\ &= \int_0^L (\mathrm{d}\psi(s)/\mathrm{d}s - \tau)\,\mathrm{d}s \\ &= 2\pi(M - L/H) \end{aligned} \tag{9}$$

where M is the closest integer to L/H and H is the helical pitch length $H = 10.5$ bps. As a result, the twist contribution is obtained as

$$P(L) = \frac{H}{\sqrt{2\pi}\,\sigma'}\mathrm{e}^{-(L-MH)^2/2\sigma'^2} \tag{10}$$

a series of Gaussian functions with $\sigma'(L) = (H/2\pi)(L/l_{\mathrm{T}})^{1/2}$ or $\log_{10}\sigma'(L) = 0.5 \times \log_{10} L - 0.9$.

This twist contribution can also be obtained as the ratio of $J_{\mathrm{TWLC}}(L)$ and $J_{(1)}(L)$. Using the analytical expressions derived by Shimada and Yamakawa (eq 73 for $J_{\mathrm{TWLC}}(L)$ and eq 74 for $J_{(1)}(L)$, as in ref 23), this ratio is calculated and is found to fit well to a series of Gaussian functions (Figure 4A). The standard deviations obtained from the fitting procedure fit well to function $\log_{10}\sigma'(L) = a\log_{10} L + b$, with $a = 0.505$ and $b = -0.931$ (Figure 4B), in close agreement with the results derived from our simple treatment. This agreement supports a similar treatment of the probabilities obtained experimentally in ref 12 as a product of contour contribution and twist contribution, $Q_{\mathrm{TC\text{-}WLC}}(L,R) = Q_{\mathrm{C\text{-}WLC}}(L,R) \times P(L)$, where contour contribution $Q_{\mathrm{C\text{-}WLC}}(L,R)$ has been evaluated earlier and twist contribution $P(L)$ is again modeled by eq 10. To better explain the experimental data, a tolerance angle of $\alpha = 0.9$ rad is introduced so that instead of requiring perfect torsional alignment, the configuration captured in experiment can allow an orientation shift with $|\psi(L) - \psi(0)| < \alpha$. Equation 9 is modified accordingly as $\gamma^* = 0$ when $|2\pi(M - L/H)| < \alpha$ and $\gamma^* = |2\pi(M - L/H)| - \alpha$ otherwise, and our results of $Q_{\mathrm{TC\text{-}WLC}}(L,6\text{ nm})$ show a clear oscillatory behavior and match the experimental measurements reasonably well (Figure 3B).

The introduction of a simple bending energy characterized by persistence length $l_{\mathrm{P}} \approx 150$ bps in the WLC model gives rise to fundamentally different physics from the FJC model and has been successful in describing the DNA flexibility at large length scales. By treating successive local bending as a Markov process, the WLC model predicts a correlation between the tangent vectors $\langle\vec{t}(s_1)\cdot\vec{t}(s_2)\rangle = \mathrm{e}^{-|s_1-s_2|/l_{\mathrm{P}}}$, which is valid only at the long chain limit. With a more generally defined bending energy (eq 3) that enables explicit consideration of the fact that at short length scales local bending is actually a non-Markov process, our C-WLC model gives rise to a new paradigm and extends the description of DNA flexibility to the biologically relevant sub-persistence-length regime. Our model shows analytically that there exists a finite length correction term l_c, leading to a contour-length-dependent tangent correlation $\langle\vec{t}(s_1)\cdot\vec{t}(s_2)\rangle = \mathrm{e}^{-|s_1-s_2|/l_{\mathrm{EP}}(L)}$ (eq 4). While our model reduces to the WLC model as $l_{\mathrm{EP}}(L)$ converges to l_{P} at long chain limit, short DNA chains show notable "softening" as l_c/L approaches 1, yielding a significant enhancement of the J factor, in quantitative

dx.doi.org/10.1021/jz501290b | J. Phys. Chem. Lett. 2014, 5, 2868−2873

agreement with existing measurements with the same l_c = 15 bps. Furthermore, the cooperative bending behavior is supported by recent experimental observations of the end-to-end distance distribution of DNA in the sub-persistence-length regime.[13]

In this study, DNA deformation is characterized by the sum of the energy directly associated with a local deformed site (self-term) and the interaction between different deformed sites (interaction term). For simplicity, the DNA system is assumed to be linear,[22] that is, the restoration forces are linearly dependent on the deformation so that each energy term can be effectively modeled as an elastic spring. Because the self-term and the interaction term originate from different interactions in nature (e.g., in the case of the major groove width deformation,[21] the self-term is associated with the dihedral angle while the interaction term is associated with base stacking), the corresponding springs can differ significantly in properties such as the spring constant and the elastic limit. According to models of DNA excitations (e.g., the kink model[19,31]), at large bending curvatures, the harmonic potential assumption breaks down for the self-term. Assuming that it is within the elastic limit for the stronger interaction term, strongly bent DNA can be described by an energy more general than eq 3, $E_{SB} = (B'/2l_0) \sum_i [f(\theta_i) + 2C\vec{b}_i \cdot \vec{b}_{i+1}/(1 + C^2)]$, where $f(\theta_i)$ is quadratic below critical curvature θ^* and becomes softer beyond. While systematic study of E_{SB} is beyond current work, it is worth noting that extending previous excitation models into the sub-persistence-length regime without modification will produce erroneous results as the use of local bend angles as normal modes without consideration of the interaction term is no longer justified. It is also worth noting that despite that our model is fundamentally different from excitation models, distinguishing their contributions to the J factor measurements may not be a simple task as short contour length coincides with strong bending when forming a DNA mini-circle. To highlight the difference, systematic studies of short DNA fragments in the weakly bending limit shall follow.

■ ASSOCIATED CONTENT

Ⓢ Supporting Information

Explicit derivations leading to the key equations in the main text are presented. In the first part, the correlated local bending distribution of $\{\vec{b}_i \equiv \theta_i \hat{n}_i\}$ is shown as the direct consequence of eq 3. Then, a detailed derivation leading to eq 4 is shown in the second part. This material is available free of charge via the Internet at http://pubs.acs.org.

■ AUTHOR INFORMATION

Corresponding Author

*E-mail: jianshu@mit.edu. Phone: +1 617 253 1563.

Notes

The authors declare no competing financial interest.

■ ACKNOWLEDGMENTS

X.L.X. would like to thank T. Avila for helpful discussions. X.L.X. and J.C. acknowledge the financial assistance of the Singapore−MIT Alliance for Research and Technology (SMART), the National Science Foundation (NSF CHE-1112825), as well as a research fellowship by the Singapore University of Technology and Design (to X.L.X.). The research work by B.J.R.T. is supported by the Singapore University of Technology and Design Start-Up Research Grant (SRG EPD 2012 022).

■ REFERENCES

(1) Richmond, T. J.; Davey, C. A. The Structure of DNA in the Nucleosome Core. *Nature* **2003**, *423*, 145−150.

(2) Lukas, J.; Bartek, J. DNA Repair: New Tales of an Old Tail. *Nature* **2009**, *458*, 581−583.

(3) Dillon, S. C.; Dorman, C. J. Bacterial Nucleoid-Associated Proteins, Nucleoid Structure and Gene Expression. *Nat. Rev. Microbiol.* **2010**, *8*, 185−195.

(4) Kim, S.; Brostromer, E.; Xing, D.; Jin, J.; Chong, S.; Ge, H.; Wang, S.; Gu, C.; Yang, L.; Gao, Y.; et al. Probing Allostery through DNA. *Science* **2013**, *339*, 816−819.

(5) Bustamante, C.; Smith, S. B.; Liphardt, J.; Smith, D. Single-Molecule Studies of DNA Mechanics. *Curr. Opin. Struct. Biol.* **2000**, *10*, 279−285.

(6) Peters, J. P.; Maher, L. J. DNA Curvature and Flexibility *In Vitro* and *In Vivo*. *Q. Rev. Biophys.* **2010**, *43*, 23−63.

(7) MacKerell, A. D.; Wiorkiewicz-Kuczera, J.; Karplus, M. An All-Atom Empirical Energy Function for the Simulation of Nucleic Acids. *J. Am. Chem. Soc.* **1995**, *117*, 11946−11975.

(8) Marko, J. F.; Siggia, E. D. Stretching DNA. *Macromolecues* **1995**, *28*, 8759−8770.

(9) Bustamante, C.; Marko, J. F.; Siggia, E. D.; Smith, S. Entropic Elasticity of λ-Phage DNA. *Science* **1994**, *265*, 1599−1600.

(10) Yang, S.; Witkoskie, J. B.; Cao, J. First-Principle Path Integral Study of DNA under Hydrodynamic Flows. *Chem. Phys. Lett.* **2003**, *377*, 399−405.

(11) Yuan, C.; Chen, H.; Lou, X. W.; Archer, L. A. DNA Bending Stiffness on Small Length Scales. *Phys. Rev. Lett.* **2008**, *100*, 018102.

(12) Vafabakhsh, R.; Ha, T. Extreme Bendability of DNA less than 100 Base Pairs Long Revealed by Single-Molecule Cyclization. *Science* **2012**, *337*, 1097−1101.

(13) Mathew-Fenn, R. S.; Das, R.; Harbury, P. A. B. Remeasuring the Double Helix. *Science* **2008**, *322*, 446−449.

(14) Kratky, O.; Porod, G. Rontgenuntersuchung Geloster Fadenmolekule. *Recl. Trav. Chim. Pays-Bas* **1949**, *68*, 1106−1122.

(15) Smith, S. B.; Finzi, L.; Bustamante, C. Direct Mechanical Measurements of the Elasticity of Single DNA Molecules by Using Magnetic Beads. *Science* **1992**, *258*, 1122−1126.

(16) Toan, N. M.; Thirumalai, D. On the Origin of the Unusual Behavior in the Strtching of Single-Stranded DNA. *J. Chem. Phys.* **2012**, *136*, 235103.

(17) Du, Q.; Smith, C.; Shiffeldrim, N.; Vologodskaia, M.; Vologodskii, A. Cyclization of Short DNA Fragments and Bending Fluctuations of the Double Helix. *Proc. Natl. Acad. Sci.U.S.A.* **2005**, *102*, 5397−5402.

(18) Yan, J.; Marko, J. F. Localized Single-Stranded Bubble Mechanism for Cyclization of Short Double Helix DNA. *Phys. Rev. Lett.* **2004**, *93*, 108108.

(19) Crick, F. H.; Klug, A. Kinky Helix. *Nature (London)* **1975**, *255*, 530−533.

(20) Wiggins, P. A.; Nelson, P. C. Generalized Theory of Semiflexible Polymers. *Phys. Rev. E* **2006**, *73*, 031906.

(21) Vologodskii, A.; Frank-Kamemetskii, M. D. Strong Bending of the DNA Double Helix. *Nucleic Acids Res.* **2013**, *41*, 6785−6792.

(22) Xu, X. L.; Ge, H.; Gu, C.; Gao, Y.; Wang, S.; Hynes, J. T.; Thio, B. J. R.; Xie, X. S.; Cao, J. Modeling Spatial Correlation of DNA Deformation: DNA Allostery in Protein Binding. *J. Phys. Chem. B* **2013**, *117*, 13378−13387.

(23) Shimada, J.; Yamakawa, H. Ring-Closure Probabilities for Twisted Wormlike Chains. Application to DNA. *Macromolecules* **1984**, *17*, 689−698.

(24) Spakowitz, A. J.; Wang, Z. G. End-to-End Distance Vector Distribution with Fixed End Orientations for the Wormlike Chain Model. *Phys. Rev. E* **2005**, *72*, 041802.

(25) Hyeon, C.; Thirumalai, D. Kinetics of Interior Loop Formation in Semiflexible Chains. *J. Chem. Phys.* **2006**, *124*, 104905.

(26) Jacobson, H.; Stockmayer, W. H. Intramolecular Reaction in Polycondensations. I. The Theory of Linear Systems. *J. Chem. Phys.* **1950**, *18*, 1600−1606.
(27) Vologodskaia, M.; Vologodskii, A. Contribution of the Intrinsic Curvature to Measured DNA Persistence Length. *J. Mol. Biol.* **2002**, *317*, 205−213.
(28) Shore, D.; Baldwin, R. L. Energetics of DNA Twisting. I. Relation between Twist and Cyclization Probability. *J. Mol. Biol.* **1983**, *170*, 957−981.
(29) Becker, N. B.; Rosa, A.; Everaers, R. The Radial Distribution Function of Worm-Like Chanis. *Eur. Phys. J. E* **2010**, *32*, 53−69.
(30) Waters, J. T.; Kim, H. D. Equilibrium Statistics of a Surface-Pinned Semiflexible Polymer. *Macromolecules* **2013**, *46*, 6659−6666.
(31) Fields, A. P.; Meyer, E. A.; Cohen, A. E. Euler Buckling and Nonlinear Kinking of Double-Stranded DNA. *Nucleic Acids Res.* **2013**, *41*, 9881−9890.